Innovative Food Science and Emerging Technologies xxx (2014) xxx–xxx

Contents lists available at ScienceDirect

Innovative Food Science and Emerging Technologies

journal homepage: www.elsevier.com/locate/ifset

Rehydration kinetics of freeze-dried carrots

F.J. Vergeldt [a,*], G. van Dalen [b], A.J. Duijster [c], A. Voda [b], S. Khalloufi [b], L.J. van Vliet [c], H. Van As [a], J.P.M. van Duynhoven [a,b], R.G.M. van der Sman [d]

[a] Laboratory of Biophysics and Wageningen NMR Centre, Department of Agrotechnology & Food Sciences, Wageningen University, Dreijenlaan 3, P.O. Box 8128, NL-6700 ET Wageningen, The Netherlands
[b] Unilever Research and Development Vlaardingen, Olivier van Noortlaan, P.O. Box 114, NL-3130 AC Vlaardingen, The Netherlands
[c] Quantitative Imaging Group, Department of Imaging Science & Technology, Delft University of Technology, Lorentzweg 1, NL-2628 CJ Delft, The Netherlands
[d] Laboratory of Food Process Engineering, Department of Agrotechnology & Food Sciences, Wageningen University, Bomenweg 2, P.O. Box 8129, NL-6700 EV Wageningen, The Netherlands

ARTICLE INFO

Article history:
Received 29 July 2013
Accepted 7 December 2013
Available online xxxx

Editor Proof Receive Date 6 January 2014

Keywords:
Pre-treatment
Freeze-drying
Rehydration kinetics
Porous microstructure
Capillary suction
Swelling

ABSTRACT

Rehydration kinetics by two modes of imbibition is studied in pieces of freeze-dried winter carrot, after different thermal pre-treatments. Water ingress at room temperature is measured in real time by in situ MRI and NMR relaxometry. Blanched samples rehydrate substantially faster compared to non-blanched samples, independent of their porous microstructure. It is proposed that for non-blanched tissues immobilized sugars result in nearly complete swelling of the solid matrix, hindering the ingress of water through the porous network. Non-blanched carrot pieces frozen at −28 °C rehydrate faster compared to those frozen at −150 °C, due to blocking of smaller pores by swelling. In blanched tissues the mobilization of sugars results in a more homogeneous sugar distribution, leading to less swelling of the solid matrix and allowing fast ingress of water via capillary suction. *Industrial relevance*: The dried fruits and vegetables that are currently available on the market are a poor compromise between convenience (rehydration kinetics) and sensorial quality. This is a major bottleneck for consumers to "*Make the Healthy Choice the Easy Choice*" and this also negatively impacts market growth. Currently, rational optimization of drying processes is impeded by lack of insight which structural features determine rehydration kinetics (convenience) and texture (sensorial quality) upon rehydration. We therefore started a program to quantitatively assess and model microstructural features and rehydration behavior of freeze-dried carrots as a model system.

1. Introduction

Fruits and vegetables (F&Vs) are an important source of (micro) nutrients (Hoffmann, Boeing, Volatier, & Becker, 2003) and sustained dietary intake has been associated with beneficial health effects (Pomerleau, Lock, & McKee, 2006). Drying of F&Vs is an important process to prolong shelf-life and provide convenience to the consumer. However, market growth is impeded by the relative poor textural quality of rehydrated F&Vs, which is not seen yet as a fair compromise with respect to convenience of preparation (Jangam, 2011).

Due to its cost-effectiveness, air drying is currently the dominating technology, although product quality is significantly compromised with respect to appearance, nutritional value and flavor. Furthermore, rehydration rates tend to be slow (Devahastin & Niamnuy, 2010; Ratti, 2001). Freeze drying yields high quality products which also rehydrate more rapidly, albeit at larger operational costs (Mujumdar & Law, 2010; Ratti, 2001). Freeze-dried F&Vs still tend to be frail and upon rehydration the texture of the native products is still not fully recovered (Marques, Prado, & Freire, 2009; Ratti, 2001).

Current approaches to understand and improve the quality of freeze-dried food products do so by balancing the rehydration rate and final texture in an empirical manner (Sagar & Kumar, 2010). A prerequisite for more rational approaches is modeling rehydration behavior of porous food materials based on physical principles (Saguy, Marabi, & Wallach, 2005). To this date, most physical modeling approaches make simplifications to the physics (Lee, Farid, & Nguang, 2006; Troygot, Saguy, & Wallach, 2011; Wallach, Troygot, & Saguy, 2011) and even more regarding the multi-scale structure (Ho et al., 2013; Ubbink, Burbidge, & Mezzenga, 2008; van der Sman & van der Goot, 2009) of F&Vs (Mebatsion, Verboven, Ho, Verlinden, & Nicolai, 2008).

In previous work a multi-scale approach was implemented using scanning electron microscopy (SEM), X-ray computerized tomography (μCT), time domain NMR (TD NMR) or relaxometry, magnetic resonance imaging (MRI) and image/data analysis methodologies to assess the porous microstructures in freeze-dried carrots (Voda et al.,

* Corresponding author at: Dreijenlaan 3, NL-6703 HA Wageningen, The Netherlands. Tel.: +31 317 485051; fax: +31 317 482725.
E-mail addresses: Frank.Vergeldt@wur.nl (F.J. Vergeldt), Gerard-van.Dalen@unilever.com (G. van Dalen), A.J.Duijster@tudelft.nl (A.J. Duijster), Adrian.Voda@unilever.com (A. Voda), Seddik.Khalloufi@unilever.com (S. Khalloufi), L.J.vanVliet@tudelft.nl (L.J. van Vliet), Henk.VanAs@wur.nl (H. Van As), John.vanDuynhoven@wur.nl, John-van.Duynhoven@unilever.com (J.P.M. van Duynhoven), Ruud.vanderSman@wur.nl (R.G.M. van der Sman).

1466-8564/$ – see front matter © 2013 Elsevier Ltd. All rights reserved.
http://dx.doi.org/10.1016/j.ifset.2013.12.002

2012). These differences are mainly determined by the thermal pre-treatments: optional blanching, freezing the sample at different temperatures, and finally the actual freeze-drying. The freezing rate affects the ice crystal size, an important factor that determines the porous microstructure: slow formation of ice crystals at −28 °C results in larger crystals, which cause large pores and a more open structure of the carrot tissue; fast freezing at −150 °C causes the formation of smaller crystals that cause less damage (van der Sman, Voda, van Dalen, & Duijster, 2013; Voda et al., 2012). The freezing rate also determines the localization of the nucleation site: slow freezing result in thermodynamically favored, extracellular nucleation leading to cell wall disruption and collapse, leaves large pores and voids in the tissue (Van Buggenhout et al., 2006); while fast freezing promotes intracellular nucleation (Mazur, 1984) with minimal disruption of the tissue architecture (Voda et al., 2012). Van der Sman et al. were able to model and quantify the impact of the freezing rate during the pre-treatment before freeze-drying on the microstructure of dried carrot (van der Sman, Voda, et al., 2013). Freezing is optionally preceded by blanching which is known to completely disrupt all membranes in carrot tissue. This causes homogenization of sugars and other solutes over the tissue before freezing (Gonzalez & Barrett, 2010), removing the distinction between either extra- or intracellular nucleation sites for ice crystals. Therefore, a blanched carrot can better accommodate intracellular ice crystal growth (van der Sman, Voda, et al., 2013).

As a follow-up work we now study the impact of the dried carrot's microstructure on the rehydration behavior. Food rehydration is commonly modeled using Fick's law, but this does not adequately reflect the situation for freeze-dried carrots where capillary flow and swelling of the solid matrix are the governing mechanisms (Saguy et al., 2005). Saguy expected effects of swelling in rehydrating freeze-dried vegetables to be minor and capillary suction to be the dominant mechanism. As in the previous study, we will study carrots where the microstructure is produced by different pre-treatments (blanched vs. non-blanched) and freezing rates at (freezing) temperatures of respectively −28 and −150 °C.

Besides the microstructure of the freeze-dried carrots we also considered whether imbibition by floating on the air–water surface or by full submerging, has an impact on the rehydration behavior. Traditionally, in rehydration experiments vegetables are fully immersed. In porous media literature, this situation is hardly studied. Here one side of a sample is immersed in a wetting fluid, while the other side is in contact with a non-wetting fluid. Via capillary suction the non-wetting fluid is displaced by the wetting fluid and escapes via the top. This process is termed co-current imbibition. On occasion a porous sample is fully immersed in a wetting fluid, but often with only one side exposed to the fluid and with other sides being sealed. Here, exchange of wetting and non-wetting fluid occurs, which flow in opposite directions. This is named counter-current imbibition — which is a slower process than co-current imbibition (Unsal, Mason, Morrow, & Rsuth, 2007).

In this study rehydration kinetics of freeze-dried carrot pieces is measured by MRI and TD NMR as a function of thermal pre-treatment. Besides the effect of microstructure we also studied the effect of the imbibition mode on the ingress of water. Results will be discussed in the framework of a physical model described elsewhere in this issue (van der Sman, Vergeldt, et al., in this issue).

2. Materials and methods

2.1. Materials

Winter carrots from local supermarkets with a diameter of 3 to 6 cm and a length of 20 to 30 cm were used to produce samples. Cylindrical samples with a diameter of 5 mm and a length of 10 mm were cut from carrot slices. In all cases cortical tissue was taken from the outer region of the slices. This tissue consists of cells with a diameter of 20 to 100 μm, depending on the age of the carrot (Voda et al., 2012). The cells are elongated in the axial direction along the root.

2.2. Methods

2.2.1. Preparation and pre-treatments of carrot pieces

Different types of thermal pre-treatment were applied before freeze-drying the carrot cylinders. Half of the samples were blanched at a temperature above 90 °C for 1 min. The cooking step was stopped by using cold water. Next, both non-blanched and blanched carrot pieces were frozen at either −28 °C or −150 °C. Finally, all cylinders were freeze-dried while the temperature was stepped from −30 °C up to 25 °C at a constant pressure of 0.4 mbar (Zirbus Technology, Germany). Twenty seven hours was required to reach 25 °C and more than 48 h was necessary at this temperature to reach less than 5% of moisture content within the samples.

All rehydration experiments were performed at room temperature. First the mass of the sample was determined with a microbalance (type 1872, Sartorius, Germany). Then carrot cylinders were added to glass sample tubes (Schott Fiolax, Schott AG, Germany) with an inner diameter of 7 mm containing just enough water to fully rehydrate the pieces, but to prevent excess free water after rehydration.

2.2.2. Rehydration of carrot pieces

All rehydration experiments were performed at room temperature. Two modes of rehydration were used: the pieces were either left floating on the air–water interface or forced to fully submerge in water using a 5 mm NMR-tube to push them down. Care was taken that the samples were only submersed by the tube but not deformed by its weight.

2.2.3. X-ray microscopic computerized tomography (μCT)

The internal porous structures of the samples were visualized using a SkyScan 1172 μCT imaging system and the ID19 beamline at the ESRF (European Radiation Synchrotron Facility) in Grenoble. The samples were imaged in plastic cylindrical sample holders with an inner diameter of 5.8 mm.

For the SkyScan 1172 μCT power settings of 60 kV and 167 μA were used. Cross sections (4000 × 4000 pixels) were obtained after tomographic reconstruction of images (4000 × 2096 pixels) acquired under different rotations over 180° with a step size of 0.20° (frame averaging = 2). For reconstruction the SkyScan NRecon program was used. The acquisition time for one projection was 1178 ms (exposure) resulting in a total acquisition and read-out time per scan of about 80 min (993 projection images/scan). A pixel size of 2.0 μm was selected. Projections were acquired under different rotations over a 180° interval with a step size of 0.20°. Samples were scanned using two scans connected in the vertical direction to increase the axial field of view (oversized scan) and subsequently merged together during reconstruction.

For the ID19 a set of horizontal cross sections was obtained after tomographical reconstruction of 1002 projection images (2048 × 2048 pixels) acquired using different rotations over 180°. An exposure time of 0.2 s was used for all projection images. The sample-detector distance was 10 mm. As detector, a FReLoN 2048 × 2048 pixel camera was used with a 10× objective. The image pixel size of 0.56 corresponds to a field of view of 1.15 × 1.15 mm^2.

2.2.4. Nuclear magnetic resonance relaxometry (TD NMR)

A Maran Ultra NMR spectrometer (0.72 T magnetic field strength, 30.7 MHz proton resonance frequency) was used, controlled by RINMR software (Resonance Instruments Ltd., Witney, United Kingdom). T_2 relaxation decay curves were recorded during rehydration of the carrot pieces by means of a standard Carr–Purcell–Meiboom–Gill

Please cite this article as: Vergeldt, F.J., et al., Rehydration kinetics of freeze-dried carrots, *Innovative Food Science and Emerging Technologies* (2014), http://dx.doi.org/10.1016/j.ifset.2013.12.002

(CPMG) pulse sequence. The CPMG decay train consisted of 16384 echoes of four data points each. The sample time between the data points in each echo was 10 μs resulting in a spectral width of 100 kHz. The time between each echo was 0.7 ms. Experiments were averaged over four scans with a repetition time of 30 s resulting in a total measurement time of 2 min. Each CPMG echo train was carefully phase corrected and each echo was reduced to one averaged data point using the IDL package (ITT Visual Information Solution., Boulder, CO USA).

T_2 measurements were analyzed by two approaches: for qualitative inspection T_2-spectra of relative intensity as a function of T_2 were determined by numerical inverse Laplace transformation as implemented in CONTIN (Provencher, 1982); for quantitative purposes the Levenberg–Marquardt non-linear least squares algorithm implemented in SPLMOD (Provencher & Vogel, 1983). The latter fits a sum of exponential decays to the echo train resulting in a relative amplitude and T_2 relaxation time constant per component.

2.2.5. Magnetic resonance imaging (MRI)

All MRI experiments were conducted on a 0.72 T (30.7 MHz for protons) imager consisting of a Bruker Avance console controlled by ParaVision 3 software (Bruker BioSpin, Karlsruhe, Germany), a Bruker electromagnet stabilized by an external ^{19}F lock unit, a home-built solenoid RF-probe with an inner diameter of 1 cm and an actively shielded gradient system with planar geometry (maximum gradient strength 1 T/m; Resonance Instruments Ltd., Witney, UK).

Rehydration of carrots was studied using a centered-out Turbo Spin Echo (TSE) imaging sequence (Scheenen, van Dusschoten, de Jager, & Van As, 2000). The advantage of centered-out TSE imaging over conventional MR-imaging is rapid acquisition at adequate resolution for short effective echo times (TE) (Hennig, Nauerth, & Friedburg, 1986). The dynamics of the rehydration processes were studied by measuring a series of MRI images to create a time-lapse image series. In case of relative slow rehydration 3D TSE imaging was used, while for faster processes a 2D TSE sequence was employed. Volumes imaged by 3D TSE had a resolution of 64 × 32 × 32 voxels of 219 μm^3 each, resulting in a field of view of 14 × 7 × 7 mm^3. The long axis of the imaged volume coincides with the axial axis of the cylindrical carrot pieces. The receiver bandwidth was 50 kHz. The center of k-space was recorded in the first echo resulting in an effective TE of 5.34 ms. A turbo factor of 32 and a repetition time of 3 s resulted in a total experiment time of 100 s. Slices imaged by 2D TSE had a thickness of 1 mm, an in-plane grid of 64 × 32 pixels with an pixel size of 219 × 219 μm^2, resulting in an in-plane field of view of 14 × 7 mm^2. The effective TE was 4.56 ms. A turbo factor of 32, signal averaging over four scans, and a repetition time of 3 s resulted in a total experiment time per image of 12 s (Mohoric et al., 2004).

2.2.6. Image analysis MRI data

For image analysis the assumptions were made that the carrot sample was fixed and no movement or swelling occurred during rehydration. The first images after the start of rehydration either by dropping the cylinder onto the air–water surface or by submerging it into the water using a weight, can be used to obtain masks. These masks identify the carrot tissue from the surrounding water. Near the top and bottom of the carrot piece the ingress of water occurs both along axial and radial direction. For the analysis only a subset of the original data was used consisting of 24 slices from the center of the carrot. By using this subset it is assumed that only radial transport of water is observed. The total intensity of the MRI signal of the external water and the carrot as a function of the time step was obtained by averaging all voxels in the corresponding mask of the subset. In the same way confidence intervals were obtained.

3. Results and discussion

3.1. Thermal pre-treatment determines the porous microstructure of freeze-dried carrot

Carrot cylinders with a diameter of 6 mm were used to study the impact of thermal pre-treatment on the microstructure of the freeze dried carrots. By using smaller carrot samples a more uniform part of the carrot could be sampled, excluding the central part (parenchyma cells). Blanched and non-blanched carrot cylinders were freeze dried at −28 °C and −150 °C. High resolution images were obtained using the ESRF SR-μCT system (data shown in the supporting material by van der Sman, Vergeldt, et al., in this issue). The freezing rate depends on the dimensions and shape of the sample, particularly thickness. Blanching before freeze drying at −150 °C resulted in smaller pores which are more homogeneously distributed (Fig. 1). During blanching membrane disruption will result in a sugar homogenization over the tissue. Therefore, a blanched carrot can better accommodate intracellular ice crystal growth and will thus suffer less structural damage. This is not necessarily valid in the case of slow cooling at −28 °C where freezing occurs extracellular and blanching may hardly have any effect. Blanching resulted in a smaller average wall size (Fig. 1). This difference in wall size is attributed to enhanced sugar mobility in blanched samples, decreasing the water holding capacity, resulting in thinner cell walls (van der Sman, Vergeldt, et al., in this issue).

3.2. Blanching enhances rehydration rate

3.2.1. Rehydration kinetics from MRI

Water ingress as a function of rehydration time in cylindrical carrot pieces at room temperature was monitored by MRI. Whenever possible, full 3D MRI was used. In case of fast processes, a faster 2D protocol was used at the expense of one spatial dimension. In Fig. 2 typical results are shown of a longitudinal slice though the center of carrot pieces with different pre-treatments and different imbibition modes. The MRI-intensity is normalized with respect to the intensity of the surrounding water. The MRI-signal intensity is proportional to the amount of water in a pixel, which relates to water density.

In Fig. 3 the 3D MRI results for non-blanched samples and the 2D MRI results for blanched samples are condensed in a plot of the overall water density as a function of the rehydration time. Only a subset of the original data was used consisting of 24 slices from the center of the carrot. By using this subset it is assumed that only radial transport of

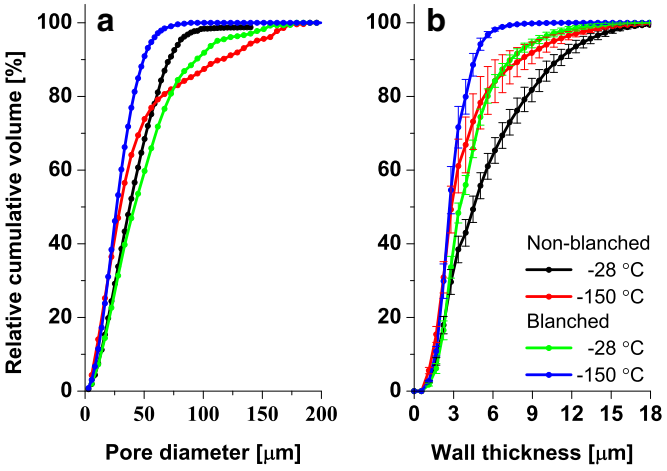

Fig. 1. The cumulative (a) pore size and (b) wall thickness distribution of freeze-dried carrots as determined from ESRF SR-μCT tomographic images. Line color indicates the thermal pre-treatment (black: non-blanched, −28 °C, green: non-blanched, −150 °C, red: blanched −28 °C, blue: blanched, −150 °C). (For interpretation of the references to color in this figure legend, the reader is referred to the web version of this article.)

Please cite this article as: Vergeldt, F.J., et al., Rehydration kinetics of freeze-dried carrots, *Innovative Food Science and Emerging Technologies* (2014), http://dx.doi.org/10.1016/j.ifset.2013.12.002

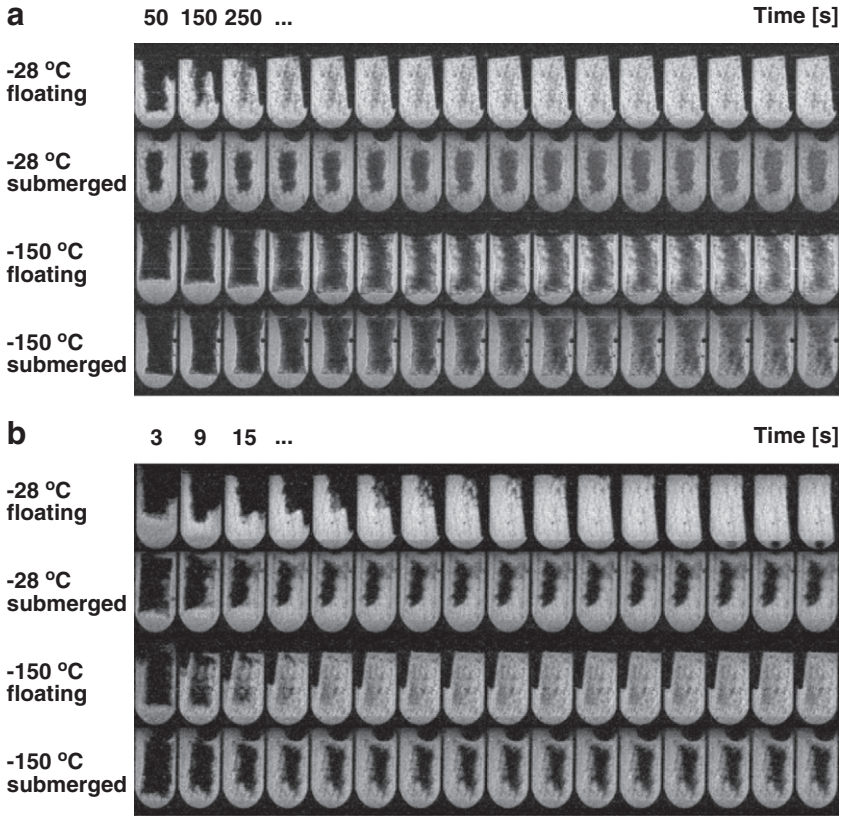

Fig. 2. (a) Longitudinal center slice from 3D MRI time series recorded during rehydration of non-blanched carrot pieces with different pre-treatments and different imbibition modes. (b) Longitudinal slice from 2D MRI time series showing the faster rehydration of blanched carrot pieces. On top the time steps are indicated.

water is observed. As can be recognized in Fig. 3 blanched freeze-dried samples rehydrate substantially faster compared to non-blanched samples: by a factor 6 compared to slow frozen samples up to a factor 60 for fast frozen non-blanched tissue. Rehydration kinetics of blanched samples is unaffected by the freezing temperature during pre-treatment.

The strong enhancement of the rehydration rate due to blanching is surprising since the microstructure is similar compared to the non-blanched samples, and thus one would expect comparable or slower rehydration kinetics compared to non-blanched samples.

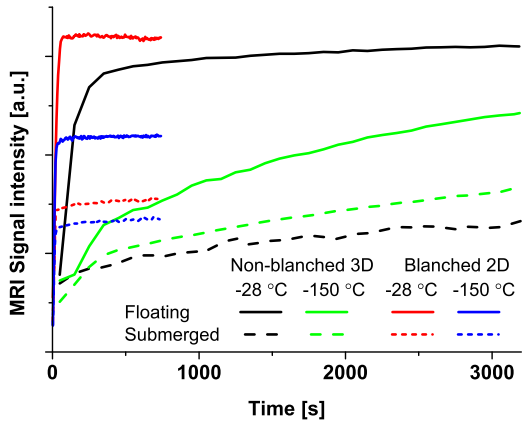

Fig. 3. Integrated intensity of 2D and 3D MR image of carrot pieces as a function of rehydration time to study the effect of pre-treatment and imbibition mode. Line color indicates the thermal pre-treatment (black: non-blanched, −28 °C, green: non-blanched, −150 °C, red: blanched −28 °C, blue: blanched, −150 °C), continues/dashed lines indicate floating/submerged imbibition, respectively. (For interpretation of the references to color in this figure legend, the reader is referred to the web version of this article.)

As stated before, blanching causes homogenization of sugars and other solutes over the tissue before freezing due to the complete disruption of all membranes in carrot tissue. This mechanism explains the better preservation of the microstructure for blanched carrot tissue (Voda et al., 2012). To account for differences in rehydration kinetics it is proposed that for non-blanched tissues immobilized sugars result in more swelling of the solid matrix, hindering the ingress of water through the pore structures. In blanched tissues this compartmentalization is lost as a result of the heat pre-treatment leading to a more homogeneous sugar distribution, leading to less swelling of the solid matrix, retaining fast ingress of water. These hypotheses are corroborated by our modeling study, also described in this issue of the journal (van der Sman, Vergeldt, et al., in this issue).

3.2.2. Rehydration kinetics from NMR relaxometry

To complement the MRI results, rehydration kinetics was also studied by non-imaging T_2 relaxometry. CPMG echo trains were analyzed as a discrete sum of exponential decays by SPLMOD, to obtain T_2 decay times and amplitudes of the different water populations. The same T_2 measurements were also analyzed by CONTIN resulting in a continuous T_2 spectrum. Careful analysis showed that a sum of four exponential decays gave the most stable results for series of measurements following the rehydration process. Here only the sum of populations of the components with the short T_2's, attributed to water that resides inside the carrot, and the component with the longest T_2, attributed to the water surrounding the carrot piece, are discussed. This assignment is based on the fact that the removal of the surrounding water resulted in complete disappearance of the component with the longest T_2. A calibration curve of known amounts of water measured by TD NMR was used to express the signal intensity of carrot water in absolute water content expressed in gram water per gram dry weight.

The same trends for the rehydration kinetics in blanched carrot tissue by MRI are observed with TD NMR: blanched samples frozen at

−28 °C and −150 °C (Fig. 4) are almost instantaneously rehydrated on the time scale accessible to TD NMR, while non-blanched samples rehydrate slower (Fig. 4). Also in Fig. 4 the water content of fresh carrot is indicated by the dashed line at 7.5 g g^{-1}. The water content in blanched samples is comparable to or even exceeds that level, indicating that the fresh product contains extracellular air. This means that air is very effectively driven out of the tissue. It is concluded that the connectivity between the pores must be high, enabling all enclosed air to escape from the tissue when driven out by water that enters the porous network due to capillary forces.

3.3. High freezing temperature enhances hydration rate of non-blanched freeze-dried carrots

3.3.1. Rehydration kinetics from MRI

From Fig. 3 we learn that a floating, non-blanched sample frozen at −28 °C (Fig. 2a) rehydrates faster, by a factor of 6, than a floating sample frozen at −150 °C (Fig. 2a). The difference in speed of water ingress between the non-blanched samples can be explained by the effect of the freezing temperature on nucleation sites and the growth of ice crystals. Although the resulting open and connected microstructure observed for slow frozen samples results in less capillary suction, swelling blocks the smaller pores of samples obtained with fast freezing rates. The overall effect of these opposing mechanisms is faster rehydration of non-blanched samples frozen at −28 °C compared to those frozen at −150 °C (van der Sman, Vergeldt, et al., in this issue).

3.3.2. Rehydration kinetics from NMR relaxometry

Water ingress in carrot as seen by T_2 relaxometry reproduces the observations by MRI: non-blanched samples frozen at −28 °C rehydrate faster than those frozen at −150 °C (Fig. 4, solid lines). After 1 h of rehydration the water content for non-blanched samples is still well below the level of fresh carrot. From this it is concluded that still a substantial amount of air must be trapped inside the carrot tissue.

3.4. Amount of trapped air is not affected by imbibition mode

3.4.1. NMR relaxometry correlates well with gravimetric analysis

In Fig. 5 the correlation is shown between the gravimetric water content and the respective carrot water content as found by MRI and T_2 relaxometry. Non-blanched samples (Fig. 5 black and green symbols) absorb less water compared to blanched samples (Fig. 5 red and blue symbols). As concluded before, air is left behind in the non-blanched carrot tissue, while for blanched samples air is driven out up to level where the water content is equals that of fresh carrot tissue, indicated by the dashed line at 7.3 g g^{-1}. While non-blanched samples frozen at −150 °C (Fig. 5 green symbols) absorb the least amount of water, blanched samples frozen at −150 °C (Fig. 5 blue symbols) absorb the most.

Since the correlation with gravimetric analysis for TD NMR (Fig. 5 squares and closed circles) is far better than for MRI (Fig. 5 diamonds), it is concluded that the observations for T_2 relaxometry reflect the actual amount of water that enters the carrot tissue during imbibition, while MRI is affected by effects that render a substantial fraction of the water unobservable.

In line with TD NMR results in Fig. 4 also no clear effect of imbibition mode can be recognized for TD NMR data in Fig. 5 (squares and closed circles).

3.4.2. Inclusion of air bubbles compromises MRI quantification of water uptake

The overall amount of water that appears to ingresses the carrot during rehydration according to MRI is substantially lower compared to TD NMR (Fig. 5). A likely explanation is entrapment of air bubbles. At air–water boundaries, strong mismatches in magnetic susceptibility exist, resulting in local magnetic field gradients that can cause significant loss of intensity in spin-echo experiments. μCT images of freeze-dried carrots that underwent imbibition for 1 h are shown in Fig. 6. These images confirm air bubble entrapment for all rehydrated samples, even those that underwent full rehydration such as blanched carrots. It was not expected that air entrapment would already manifest themselves at a magnetic field strength as low as 0.72 T, although comparable effects have been observed for mushrooms (Donker, Van As, Edzes, & Jans, 1996). Confirmation that loss of magnetization can be attributed local magnetic field gradients is provided by CMPG experiments with short (TE = 0.7 ms) and long (TE = 5 ms). As is shown in Fig. 5 indeed significant intensity loss occurs, leading to underestimated water contents for long (open circles) compared to short (closed circles) echo times. For MRI experiments intensity loss is much stronger. The relation between local water content and image intensities in RARE experiments is intricate (Hennig et al., 1986; Mohoric et al., 2004). Thus we

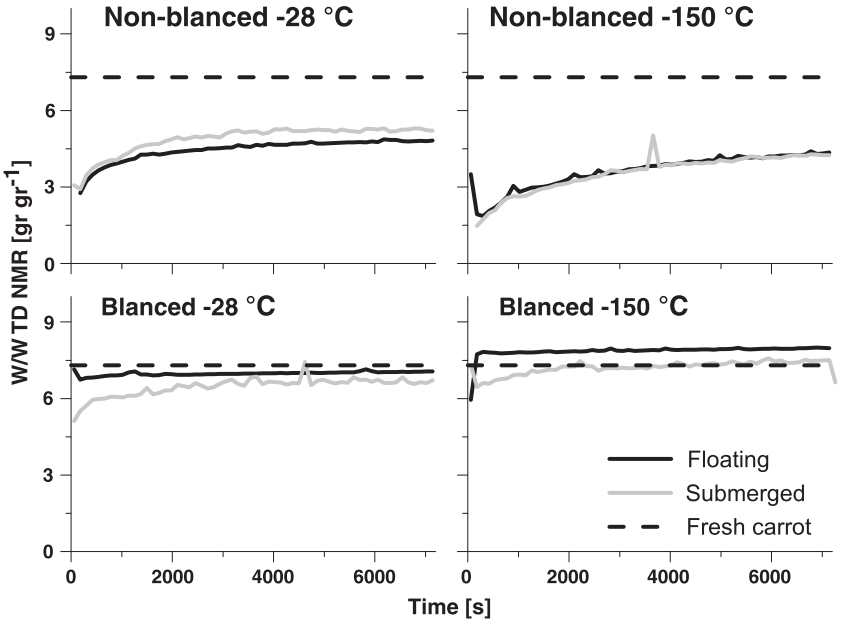

Fig. 4. Water content as a function of the rehydration time as determined by TD NMR.

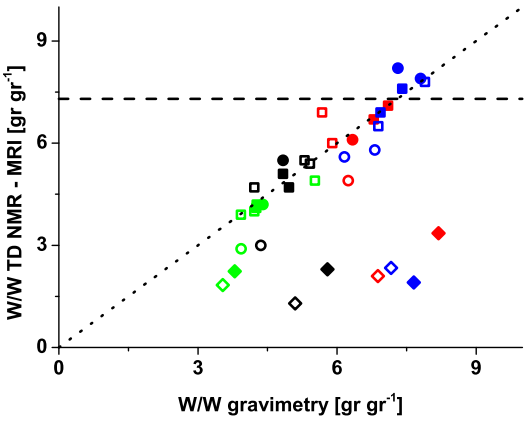

Fig. 5. Correlation between the gravimetric water content of carrot pieces after rehydration and the water content as determined by respectively TD NMR and MRI. The dashed line indicates the water content of fresh carrot. The dotted line indicates 1:1 correlation. The symbol type indicates the type of measurement (■ TD NMR, TE = 0.7 ms, ● TD NMR TE = 5 ms, ♦ MRI, 5 ms), close/open symbols indicate floating/submerged imbibition, respectively. Colors indicate the thermal pre-treatment (black: non-blanched, −28 °C, green: non-blanched, −150 °C, red: blanched −28 °C, blue: blanched, −150 °C). (For interpretation of the references to color in this figure legend, the reader is referred to the web version of this article.)

refrained from further quantification attempts to quantify water ingress by MRI.

3.5. Imbibition mode affects air bubble entrapment

Both gravimetric analysis and TD NMR with short echo times (Fig. 5 squares), show no clear effect of the imbibition mode on water uptake. From this it was concluded before that there is no significant difference in the amount of trapped air. The submerged carrot samples measured by TD NMR with a long TE (Fig. 5 open circles) however deviate from the correlation with gravimetric analysis, while the floating samples (Fig. 5 closed circles) measured with same parameters correlate as good as all samples measured with a short TE. Also for the MRI results the same trends can be recognized (compare the closed diamonds to the open ones in Fig. 5). These observations are in line with air entrapment as observed in μCT images of freeze-dried carrots that were rehydrated in different imbibition modes (Fig. 6). The larger air bubbles trapped in submerged carrots are apparently much more effective in causing strong local field gradients compared to the smaller ones trapped in floating carrots.

3.6. No effect of porous microstructure on sugar leaching

The T_2 of the component with the longest transverse relaxation time, which is assigned to the water surrounding the carrot pieces, decreased slowly in time for all samples. In Fig. 7 the relaxivity is presented, as derived from the T_2 and relative population of this component. The increase of relaxivity of the surrounding water is explained by leaching of sugars and other solutes from the carrot. It is well known that carrot tissue contains a high amount of sugar. There is no clear difference in the time dependence of leaching of solutes, neither for the pre-treatment of the carrot pieces nor for the imbibition mode. Compared to the rehydration dynamics demonstrated in Figs. 2, 3 and 4, the leaching is 1–2 orders of magnitude slower. The final relaxivity is less for blanched samples compared to non-blanched samples, by a factor 2 for samples frozen at −28 °C and a factor 1.2 for samples frozen at −150 °C.

Whereas significant differences could be observed in water ingress for the different freeze-dried carrots, this was not reflected in the slower leaching behavior as observed by TD NMR. We conclude that the different porous microstructures of the freeze-dried carrots induce different water ingress behavior, but this does not affect the slow leaching of solutes from the tissue.

3.7. Interpretation of results with pore-scale model

Most of the observed trends found in our experiments can be explained via the pore-scale model, describing all the physical phenomena involved in the imbibition, as described in the accompanying paper (van der Sman, Vergeldt, et al., in this issue). The most striking result is the much faster rehydration rate of blanched samples versus non-blanched samples. The pore-scale model shows that the assumption of immobile solutes in the non-blanched samples leads to a competition between swelling and capillary suction. In pores with relatively small diameters (about 30 μm and smaller) the swelling wins from the capillary suction, leading to near complete swelling and consequently to slowing down of the rehydration and entrapment of air. Rehydration is now driven by moisture diffusion in the solid phase, whose time scale is in the order of 2000 s, which is comparable with our experimental observations. Our model is yet not sufficiently detailed for explanation of the differences in the amounts of trapped air.

Experimental observations to support the difference in swelling between blanched and non-blanched tissues are the diminished cell wall thickness shown in Fig. 1 as a result of a reduced water holding capacity for blanched tissue. Furthermore the extend of swelling of blanched tissue due to rehydration by a saturated vapor is found to be reduced compared to non-blanched tissue as observed by μCT (van der Sman, Vergeldt, et al., in this issue).

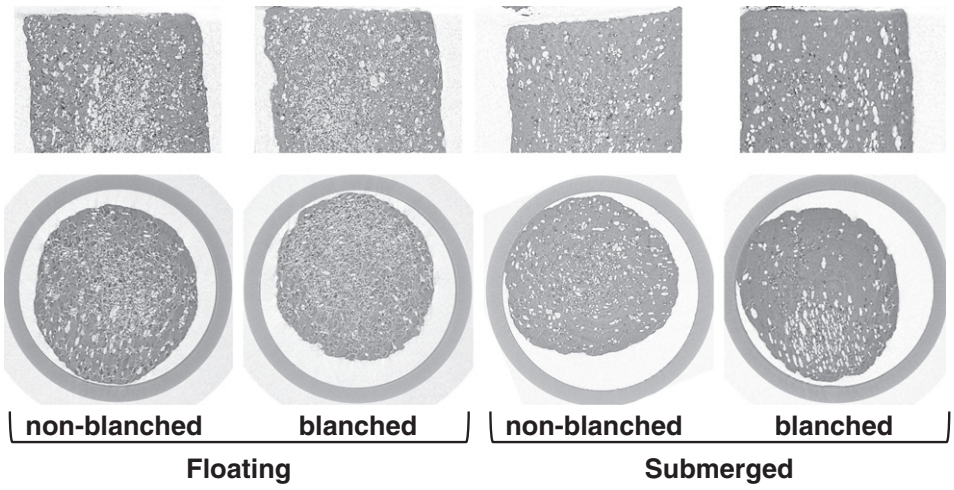

Fig. 6. μCT images of freeze-dried carrot tissue frozen at −28 °C with/without blanching pre-treatment and rehydrated for 1 h in floating and submerged conditions.

Please cite this article as: Vergeldt, F.J., et al., Rehydration kinetics of freeze-dried carrots, *Innovative Food Science and Emerging Technologies* (2014), http://dx.doi.org/10.1016/j.ifset.2013.12.002

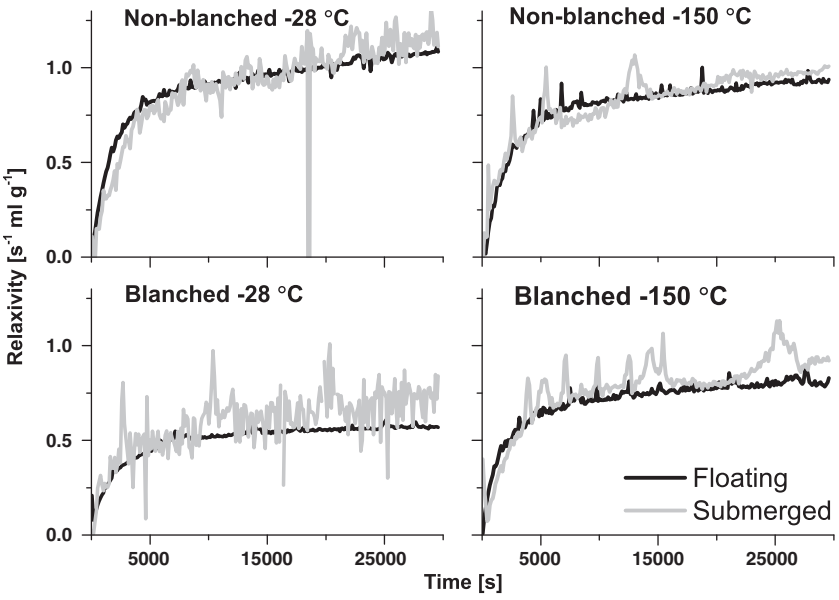

Fig. 7. Dependence of the relaxivity of water surrounding the carrot pieces on the rehydration time due to leaching of carbohydrates and other solutes.

In blanched samples the solutes are assumed to be mobile, due to the loss of membrane integrity during blanching. During rehydration, solutes leach into the capillary water, which reduces the swelling capacity of the cell wall material with about 50%. Consequently, capillary suction occurs unhindered, within the expected timescale of several seconds.

The second trend, that we have observed, is the minor difference in rehydration rates between floating samples and fully immersed samples. In the modeling paper we discuss that initially in immersed samples gas bubbles will escape at the top of the sample, with bubble size several times larger than the pore size. Consequently, the capillary pressure of the gas–water interface will be small, and the physics is comparable with that of floating samples — where the imbibition is co-current.

Furthermore, we have observed small, but significantly different rehydration rate between (non-blanched) samples frozen at different rates (rendering different pore sizes). Capillary suction is faster for samples with smaller pores, but also the chance of its obstruction by swelling is larger. Apparently, the swelling is more severe in the fast-frozen samples at −150 °C — also evident in the amount of trapped air.

Finally, the slow leaching of sugars out of the product agrees with its large time scale, that we have estimated in the accompanying paper. This time scale is assumed to be dependent only on the size of the sample, and no differences are expected between treatments — as is observed.

4. Conclusion

It is proposed that immobilization of sugars in non-blanched samples retains the swelling capacity of the solid matrix leading to severe swelling. This swelling hinders or even blocks the ingress of water via capillary suction into the porous network. In blanched samples the mobility of solutes and subsequently leaching, lowers the swelling capacity significantly, leaving the pore network open for capillary suction. Freeze-drying leads to a high connectivity of the pore structure, enabling rehydration within several seconds.

Leaching of solutes out of the carrot tissue is a slow and solely diffusion-driven process, independent of the microstructure of the freeze-dried carrots.

Acknowledgments

The authors would like to acknowledge Martin Koster for μCT imaging. This work was supported by the Dutch Food and Nutrition Delta program (project FND080078U).

References

Devahastin, S., & Niamnuy, C. (2010). Modelling quality changes of fruits and vegetables during drying: A review. *International Journal of Food Science and Technology*, *45*(9), 1755–1767.

Donker, H. C. W., Van As, H., Edzes, H. T., & Jans, A. W. H. (1996). NMR imaging of white button mushroom (*Agaricus bisporis*) at various magnetic fields. *Magnetic Resonance Imaging*, *14*(10), 1205–1215.

Gonzalez, M. E., & Barrett, D.M. (2010). Thermal, high pressure, and electric field processing effects on plant cell membrane integrity and relevance to fruit and vegetable quality. *Journal of Food Science*, *75*(7), R121–R130.

Hennig, J., Nauerth, A., & Friedburg, H. (1986). RARE imaging: A fast imaging method for clinical MR. *Magnetic Resonance in Medicine*, *3*, 823–833.

Ho, Q. T., Carmeliet, J., Datta, A. K., Defraeye, T., Delele, M.A., Herremans, E., et al. (2013). Multiscale modeling in food engineering. *Journal of Food Engineering*, *114*(3), 279–291.

Hoffmann, K., Boeing, H., Volatier, J. L., & Becker, W. (2003). Evaluating the potential health gain of the World Health Organization's recommendation concerning vegetable and fruit consumption. *Public Health Nutrition*, *6*(8), 765–772.

Jangam, S. V. (2011). An overview of recent developments and some R&D Challenges related to drying of foods. *Drying Technology*, *29*(12), 1343–1357.

Lee, K. T., Farid, M., & Nguang, S. K. (2006). The mathematical modelling of the rehydration characteristics of fruits. *Journal of Food Engineering*, *72*(1), 16–23.

Marques, L. G., Prado, M. M., & Freire, J. T. (2009). Rehydration characteristics of freeze-dried tropical fruits. *LWT - Food Science and Technology*, *42*(7), 1232–1237.

Mazur, P. (1984). Freezing of living cells: Mechanisms and implications. *American Journal of Physiology*, *247*(3), C125–C142.

Mebatsion, H. K., Verboven, P., Ho, Q. T., Verlinden, B. E., & Nicolai, B.M. (2008). Modelling fruit (micro)structures, why and how? *Trends in Food Science & Technology*, *19*(2), 59–66.

Mohoric, A., Vergeldt, F., Gerkema, E., de Jager, A., van Duynhoven, J., van Dalen, G., et al. (2004). Magnetic resonance imaging of single rice kernels during cooking. *Journal of Magnetic Resonance*, *171*(1), 157–162.

Mujumdar, A. S., & Law, C. L. (2010). Drying technology: Trends and applications in postharvest processing. *Food and Bioprocess Technology*, *3*(6), 843–852.

Pomerleau, J., Lock, K., & McKee, M. (2006). The burden of cardiovascular disease and cancer attributable to low fruit and vegetable intake in the European Union: Differences between old and new Member States. *Public Health Nutrition*, *9*(5), 575–583.

Provencher, S. W. (1982). A constrained regularization method for inverting data represented by linear algebraic or integral equations. *Computer Physics Communications*, *27*(3), 213–227.

Provencher, S. W., & Vogel, R. H. (1983). Regularization techniques for inverse problems in molecular biology. In P. Deuflhard, & E. Hairer (Eds.), *Numerical treatment of inverse problems in differential and integral equations* (pp. 304–319). Boston: Birkhauser.

Ratti, C. (2001). Hot air and freeze-drying of high-value foods: A review. *Journal of Food Engineering*, *49*(4), 311–319.

Sagar, V. R., & Kumar, S. P. (2010). Recent advances in drying and dehydration of fruits and vegetables: A review. *Journal of Food Science and Technology-Mysore*, *47*(1), 15–26.

Saguy, I. S., Marabi, A., & Wallach, R. (2005). New approach to model rehydration of dry food particulates utilizing principles of liquid transport in porous media. *Trends in Food Science & Technology*, *16*(11), 495–506.

Scheenen, T. W. J., van Dusschoten, D., de Jager, P. A., & Van As, H. (2000). Microscopic displacement imaging with pulsed field gradient turbo spin-echo NMR. *Journal of Magnetic Resonance*, *142*(2), 207–215.

Please cite this article as: Vergeldt, F.J., et al., Rehydration kinetics of freeze-dried carrots, *Innovative Food Science and Emerging Technologies* (2014), http://dx.doi.org/10.1016/j.ifset.2013.12.002

Troygot, O., Saguy, I. S., & Wallach, R. (2011). Modeling rehydration of porous food materials: I. Determination of characteristic curve from water sorption isotherms. *Journal of Food Engineering*, *105*(3), 408–415.

Ubbink, J., Burbidge, A., & Mezzenga, R. (2008). Food structure and functionality: A soft matter perspective. *Soft Matter*, *4*(8), 1569–1581.

Unsal, E., Mason, G., Morrow, N. R., & Ruth, D. W. (2007). Co-current and counter-current imbibition in independent tubes of non-axisymmetric geometry. *Journal of Colloid and Interface Science*, *306*(1), 105–117.

Van Buggenhout, S., Lille, M., Messagie, I., Van Loey, A., Autio, K., & Hendrickx, M. (2006). Impact of pretreatment and freezing conditions on the microstructure of frozen carrots: Quantification and relation to texture loss. *European Food Research and Technology*, *222*(5–6), 543–553.

van der Sman, R. G. M., & van der Goot, A. J. (2009). The science of food structuring. *Soft Matter*, *5*(3), 501–510.

van der Sman, R. G. M., Vergeldt, F. J., Van As, H., Van Dalen, G., Voda, A., & Van Duynhoven, J. P.M. (in this issue). Multiphysics pore-scale model for the rehydration of porous food. *Innovative Food Science & Emerging Technologies* (in this issue).

van der Sman, R. G. M., Voda, A., van Dalen, G., & Duijster, A. (2013). Ice crystal interspacing in frozen foods. *Journal of Food Engineering*, *116*(2), 622–626.

Voda, A., Homan, N. M., Witek, M. M., Duijster, A., van Dalen, G., Van der Sman, R. G. M., et al. (2012). The impact of freeze-drying on microstructure and rehydration properties of carrot. *Food Research International*, *49*(2), 687–693.

Wallach, R., Troygot, O., & Saguy, I. S. (2011). Modeling rehydration of porous food materials: II. The dual porosity approach. *Journal of Food Engineering*, *105*(3), 416–421.

Please cite this article as: Vergeldt, F.J., et al., Rehydration kinetics of freeze-dried carrots, *Innovative Food Science and Emerging Technologies* (2014), http://dx.doi.org/10.1016/j.ifset.2013.12.002